arXiv:1406.7593v1 [cond-mat.supr-con] 30 Jun 2014

Lattice distortion and stripe-like antiferromagnetic order in $Ca_{10}(Pt_3As_8)(Fe_2As_2)_5$

A. Sapkota,[1,2] G. S. Tucker,[1,2] M. Ramazanoglu,[1,2] W. Tian,[3] N. Ni,[4,5]
R. J. Cava,[5] R. J. McQueeney,[1,2,6] A. I. Goldman,[1,2] and A. Kreyssig[1,2]

[1]*Ames Laboratory, U. S. DOE, Ames, Iowa 50011, USA*
[2]*Department of Physics and Astronomy, Iowa State University, Ames, Iowa 50011, USA*
[3]*Quantum Condensed Matter Division, Oak Ridge National Laboratory, Oak Ridge, Tennessee 37831, USA*
[4]*Department of Physics and Astronomy, University of California, Los Angeles, California 90095, USA*
[5]*Department of Chemistry, Princeton University, Princeton, New Jersey 08544, USA*
[6]*Oak Ridge National Laboratory, Oak Ridge, Tennessee 37831, USA*

(Dated: July 1, 2014)

$Ca_{10}(Pt_3As_8)(Fe_2As_2)_5$ is the parent compound for a class of Fe-based high-temperature superconductors where superconductivity with transition temperatures up to 30 K can be introduced by partial element substitution. We present a combined high-resolution high-energy x-ray diffraction and elastic neutron scattering study on a $Ca_{10}(Pt_3As_8)(Fe_2As_2)_5$ single crystal. This study reveals the microscopic nature of two distinct and continuous phase transitions to be very similar to other Fe-based high-temperature superconductors: an orthorhombic distortion of the high-temperature tetragonal Fe-As lattice below $T_S = 110(2)$ K followed by stripe-like antiferromagnetic ordering of the Fe moments below $T_N = 96(2)$ K. These findings demonstrate that major features of the Fe-based high-temperature superconductors are very robust against variations in chemical constitution as well as structural imperfection of the layers separating the Fe-As layers from each other and confirms that the Fe-As layers primarily determine the physics in this class of material.

PACS numbers: 74.70.Xa, 75.25.-j, 61.50.Ks, 75.30.Kz

In early 2011, a new class of Fe-based high-temperature superconductors was discovered, the $Ca_{10}(Pt_3As_8)(Fe_{2-x}Pt_xAs_2)_5$ (10-3-8) and $Ca_{10}(Pt_4As_8)(Fe_{2-x}Pt_xAs_2)_5$ (10-4-8) compounds.[1–3] The parent 10-4-8 compound shows superconductivity with a transition temperature $T_c \sim 38$ K[1,4] which can be suppressed by applied pressure or chemical doping.[4–6] In the partner system, the parent 10-3-8 compound is non-superconducting. However, superconductivity can be induced by partial element substitution of Fe by Pt with T_c values up to 14 K,[1–4,6–9] by partial substitution of Ca by La with maximum T_c of 30 K,[4,10,11] or by applied pressure.[12] Varying the Pt concentration in either compound yields charge doping in the $(Fe_{2-x}Pt_xAs_2)_5$ (Fe-As) layers[2,3,13] and in the $Pt_{3+y}As_8$ or $Pt_{4+y}As_8$ (Pt-As) layers.[3,4] Recently, the 10-3-8 and 10-4-8 class expanded with the discovery of $(Ca_{1-x}La_x)_{10}(Pd_3As_8)(Fe_{2-y}Pd_yAs_2)_5$ and $Ca_{10}(Ir_4As_8)(Fe_2As_2)_5$ compounds with T_c values up to 17 K and 16 K, respectively. Their crystal and electronic structures are almost identical to their 10-3-8 and 10-4-8 elder sibling compounds.[14,15]

The crystal structures of both 10-3-8 and 10-4-8 compounds share a common feature with other families of Fe-based high-temperature superconductors: a stacking of Fe-As layers with equivalent arrangement and electronic configuration to that in the parent $BaFe_2As_2$ and LaFeAsO compounds.[1–5] However, there are several distinguishing structural features of the 10-3-8 and 10-4-8 compounds: (i) the Fe-As layers are separated by slightly puckered Pt-As layers and Ca planes, yielding a much larger separation of the Fe-As layers, approximately 10.3 Å; (ii) the arrangement of atoms in the Pt-As layers leads to chemical structures with lower symmetries than found in other Fe-based high-temperature superconductors, triclinic $P\,\overline{1}$ for the 10-3-8 compound, and tetragonal $P\,4/n$, monoclinic $P\,2_1/n$, or triclinic $P\,\overline{1}$ for the 10-4-8 compound in different structure studies;[1–4] (iii) imperfections in the chemical structure have been observed by diffuse scattering and streaking of spots in x-ray diffraction studies[2,3] that are interpreted as resulting mainly from stacking disorder of the Pt-As layers.

Beyond these structural differences, the physical properties of 10-3-8 and 10-4-8 compounds are very reminiscent of other Fe-based high-temperature superconductors. For example, angle-resolved photoemission studies supported by band-structure and phonon-spectra calculations have shown that the electronic structure is quite similar to that observed for $BaFe_2As_2$.[16–20] Inelastic neutron scattering measurements on large single crystals[21,22] demonstrated that magnetic fluctuations occur at the same stripe-like antiferromagnetic wave vector as observed in other Fe-based high-temperature superconductors. However, no indication of magnetic order could be found – likely related to the high Pt content[21,22] and the reported inhomogeneity in one of the samples.[22] Furthermore, in resistance measurements on $Ca_{10}(Pt_3As_8)(Fe_2As_2)_5$ single crystals, Ni *et al.*[10] and Gao *et al.*[12] found two features that they interpreted as a structural transition at $T_1 = 103$ K and a magnetic transition at $T_2 = 95$ K. The presence of a structural transition is consistent with the observation of domain patterns in polarized-light images due to a lowering of the lattice symmetry at low temperatures,[7] and recent high-resolution x-ray diffraction experiments on powder samples.[23] Susceptibility measurements on a powder

sample,[5] muon spin-resonance (μSR) measurements on powder samples,[23] and ^{75}As nuclear magnetic resonance (NMR) measurements on a single crystal[24] showed features interpreted as an onset of antiferromagnetic order below 120 K for powder samples and below 100 K for single crystals, respectively. Nevertheless, there are indications of a strong sensitivity of physical properties to different sample preparation routes, *e. g.*, in specific heat measurements. Whereas the observed jump at T_c is much smaller for superconducting polycrystalline material[11] than one would expect from the almost universal behavior in Fe-based high-temperature superconductors,[25] it follows the anticipated behavior much more closely for single crystals.[10]

Previous microscopic studies have been performed, for the most part, on different samples and it is difficult to compare and correlate the structural and magnetic properties due to variances in sample preparation and the apparent wide spread of properties.[1–5,23] Therefore, important questions concerning the properties of 10-3-8 and 10-4-8 compounds remain unanswered. Which phase transitions are intrinsic to homogeneous single-phase samples and what is their nature? In particular, are the structural and magnetic transitions similar to lattice distortions and antiferromagnetic ordering observed in other Fe-based high-temperature superconductors? Are these phase transitions coupled and discontinuous (1$^{\rm st}$ order) or continuous (2$^{\rm nd}$ order)?

Here we present a combined high-resolution high-energy x-ray diffraction and elastic neutron scattering study to answer most of the aforementioned questions on a microscopic level in an unambiguous manner by performing measurements on the same, homogenous $Ca_{10}(Pt_3As_8)(Fe_2As_2)_5$ single crystal. We find two distinct and continuous phase transitions: an orthorhombic distortion of the high-temperature square-like Fe lattice followed by a stripe-like antiferromagnetic ordering of the Fe moments at slightly lower temperature.

A $Ca_{10}(Pt_3As_8)(Fe_2As_2)_5$ single crystal of dimension $2\times2\times0.2\,\mathrm{mm}^3$ was prepared by solution growth[2] and was characterized as described in Ref. 7. Herein, we disregard the very small partial element substitution of 0.4% Pt for Fe for similarly prepared samples.[7,12,24] The high-resolution high-energy x-ray diffraction study was performed at station 6-ID-D at the Advanced Photon Source, Argonne National Laboratory. The use of x-rays with an energy of 100.5 keV minimizes sample absorption and allows us to probe the entire bulk of the sample. The sample was mounted on a Cu post in the center of a Be sample can filled with He exchange gas, a Be heat shield, and a Be vacuum shroud, all in an APD He closed cycle cryostat. Extended regions of selected reciprocal lattice planes were recorded by a MAR345 image plate system positioned 1497 mm behind the sample as the sample was rocked through two independent angles up to $\pm3.2^\circ$ about axes perpendicular to the incident beam with a size of $0.1\times0.1\,\mathrm{mm}^2$.[26] High-resolution images were measured by employing a ScintX area detector positioned 2713 mm behind the sample while rocking one of these angles after aligning the selected Bragg peak of interest. The elastic neutron-scattering measurements were performed on the HB-1A fixed incident energy (14.6 meV) triple-axis spectrometer at the High Flux Isotope Reactor, Oak Ridge National Laboratory using two pyrolytic graphite filters and 48'-48'-40'-80' collimation. The same sample employed in the x-ray diffraction study was wrapped in Al foil and mounted on an Al sheet at the center of an Al sample can filled with He exchange gas, an Al heat shield, and an Al vacuum shroud, all in a He closed cycle cryostat. The (H H L) plane was selected as scattering plane in the body-centered tetragonal pseudo-symmetric coordinate system defined below.

Figure 1(a) shows the high-energy x-ray diffraction pattern of the (H K 0) reciprocal lattice plane recorded at $T = 120$ K well above all reported phase transition temperatures. Two families of resolution-limited Bragg peaks of the $Ca_{10}(Pt_3As_8)(Fe_2As_2)_5$ single crystal have been observed: (i) strong Bragg peaks on a large square-like reciprocal lattice related to the dimensions and geometry of the Fe-As layers, and (ii) weaker Bragg peaks with a smaller square-like reciprocal lattice related to the complex Pt_3As_8 layer structure with its in-plane triclinic unit cell that is essentially a $\sqrt{5}\times\sqrt{5}$ superlattice forming along the [2 1 0] direction of the tetragonal cell defined by the Fe-As layers. This results in an in-plane inclusion angle of $\arctan\frac{1}{2} = 26.56^\circ$ and a length relation $a = \sqrt{5}a_0$ between the two lattices.[2,16] We employ the description of the chemical structure and the reciprocal space in terms of a body-centered tetragonal unit cell common to other Fe-based high-temperature superconductors with lattice parameters $a_0 = 3.912$ Å and $c_0 = 20.58$ Å related to the base structure built by the Fe-As layers and Ca planes as illustrated in Fig. 1 in Ref. 16. This structure and lattice yield the strong Bragg peaks depicted in (i). The additional weaker Bragg peaks (ii) in Fig. 1(a) arise from the complex Pt_3As_8 layer structure and will be described as superstructure hereafter. We note that only one of the possible two orientations of the Pt_3As_8 superstructure relative to the Fe-As base structure is observed for the entire sample.

The diffraction pattern of the (H 0 L) reciprocal lattice plane shown in Fig. 1(b) was recorded in the same manner as that in Fig. 1(a) after rotating the sample by -90° around the [1 0 0] direction. Only resolution limited Bragg peaks related to the body-centered tetragonal unit cell are observed. This is in contrast to the diffraction pattern shown in Fig. 1(c) where the sample was rotated such that the [0 0 1] direction was still vertical and the $[2\,2\,0]_{Pt_3As_8}$ marked direction in Fig. 1(a) was horizontal. The strong resolution limited Bragg peaks along the [0 0 1] direction are associated with the base structure. The additional streak-like diffraction features arise from the Pt_3As_8 superstructure, indicating significant disorder along the **c** direction in contrast to a well-ordered structure in the (**a** **b**) plane. This disorder appears to be static as demonstrated by very similar features in the measure-

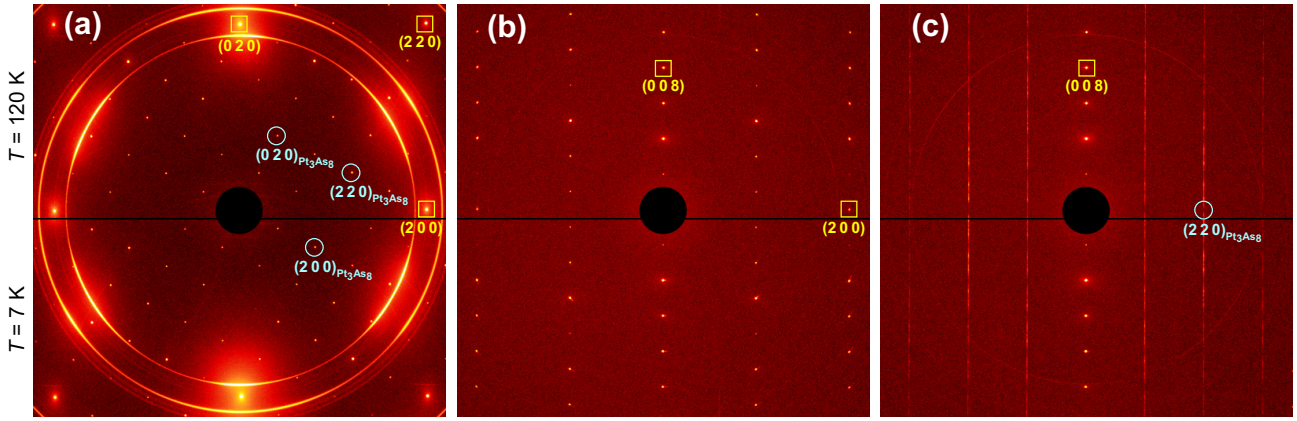

FIG. 1: (Color online) High-energy x-ray diffraction patterns of the $Ca_{10}(Pt_3As_8)(Fe_2As_2)_5$ single crystal measured by the method described in the text. Reciprocal lattice plane recorded (a) with the incident x-ray beam perpendicular to the plate-like crystals, (b) after rotating the sample by -90° around the horizontal axis in (a), and (c) after rotating the sample by -18.44° around the vertical axis in (b). The lower halves of the patterns were measured at $T = 7\,\mathrm{K}$ and the upper halves at $T = 120\,\mathrm{K}$. Selected Bragg peaks related to the body-centered tetragonal base structure built by the Fe-As layers and Ca planes are marked with squares. Circles depict selected Bragg peaks related to the Pt_3As_8 superstructure. The ring-like scattering features are caused by the Cu-sample holder and the Be domes.

ments at $T = 120\,\mathrm{K}$ in the upper halves of Fig. 1 and at $T = 7\,\mathrm{K}$ in the lower halves of Fig. 1. Additional measurements at $T = 20\,\mathrm{K}$, 40 K, 60 K, 80 K, and 100 K yield similar features in the diffraction patterns and support this interpretation.

However, qualitative changes are observed in the $(H\,K\,0)$ plane diffraction patterns measured at $T = 100\,\mathrm{K}$ and below; in particular, the Bragg peaks split or show significant broadening observable in the high-resolution patterns shown in the inset in Fig. 2(a) measured at different positions on the sample. For the spots labeled A and C, a splitting of the single high-temperature (2 2 0) Bragg peak into a pair of peaks is observed at $T = 100\,\mathrm{K}$, which evolves in separation and shape down to $T = 7\,\mathrm{K}$. The (2 2 0) Bragg peak splits into four peaks at spot B which can be explained in terms of the tetragonal-to-orthorhombic distortion of the base structure and the arising domain structure previously reported for $BaFe_2As_2$ and GdFeAsO.[27,28] This is in excellent agreement with the analysis of similar diffraction patterns in these compounds.[27–30] The diffraction patterns at spots A-C are similar to spots A-C shown in Figs. 2 and 3 in Ref. 27 considering the 45° rotated detector orientation between the two measurements. This demonstrates a similar order of magnitude for the size of the orthorhombic distorted domains in $Ca_{10}(Pt_3As_8)(Fe_2As_2)_5$ as in $BaFe_2As_2$, in agreement with the similarity in polarized light-microscopic pictures observed in both compounds.[7,27] The detailed temperature dependence is similar for all three sample spots A-C in $Ca_{10}(Pt_3As_8)(Fe_2As_2)_5$, demonstrating a high degree of homogeneity across the entire sample.

Based on the occurrence of a lattice distortion in $Ca_{10}(Pt_3As_8)(Fe_2As_2)_5$ similar to that observed in $BaFe_2As_2$ and GdFeAsO, the question arises as to whether the magnetic order of the Fe moments is also similar, *i. e.*, a stripe-like arrangement in the (**a b**) plane. Indeed, magnetic Bragg peaks could be found at several positions $(\frac{u}{2}\,\frac{v}{2}\,w)$ with u and v = odd and w = even in our neutron diffraction study as shown in the left inset in Fig. 2(b). An intensive search for magnetic Bragg peaks at positions $(\frac{u}{2}\,\frac{v}{2}\,w)$ with u, v, and w = odd performed around $(\frac{1}{2}\,\frac{1}{2}\,1)$, $(\frac{1}{2}\,\frac{1}{2}\,3)$, $(\frac{1}{2}\,\frac{1}{2}\,5)$, and $(\frac{1}{2}\,\frac{1}{2}\,7)$ failed to observe any Bragg peaks above a background level of 33 counts in 3 min at $T = 6\,\mathrm{K}$. The observation of magnetic Bragg peaks related to the propagation vector $(\frac{1}{2}\,\frac{1}{2}\,0)$ and the absence of peaks related to the propagation vector $(\frac{1}{2}\,\frac{1}{2}\,1)$ points to an antiferromagnetic arrangement of the Fe moments along the [1 1 0] direction and ferromagnetic arrangements in both perpendicular directions. A similar stripe-like ordering in the Fe layers with ferromagnetic arrangement between the layers was observed, *e. g.*, in CeFeAsO, PrFeAsO, and NdFeAsO.[31–33] The antiferromagnetic Bragg peaks shown in the left inset in Fig. 2(b) are very weak when the scattering vector direction is close to the [1 1 0] direction and become stronger with increasing angle between both directions despite Lorentz-factor influence and potential structure factor effects. In addition, no Bragg peak could be found above background at the $(\frac{1}{2}\,\frac{1}{2}\,0)$ position. Both observations together demonstrate that the antiferromagnetically ordered Fe moments are primarily collinearly aligned along the [1 1 0] direction. From the similar shape and half width of the magnetic and nuclear Bragg peaks as shown in the insets in Fig. 2(b) we conclude that the antiferromagnetic order is long-range in nature.

In the following discussion, the temperature dependence of both ordering phenomena is elucidated. The value of $\delta = (a_{\mathrm{OR}} - b_{\mathrm{OR}})/(a_{\mathrm{OR}} + b_{\mathrm{OR}})$ is used as the order parameter for the observed orthorhombic lattice

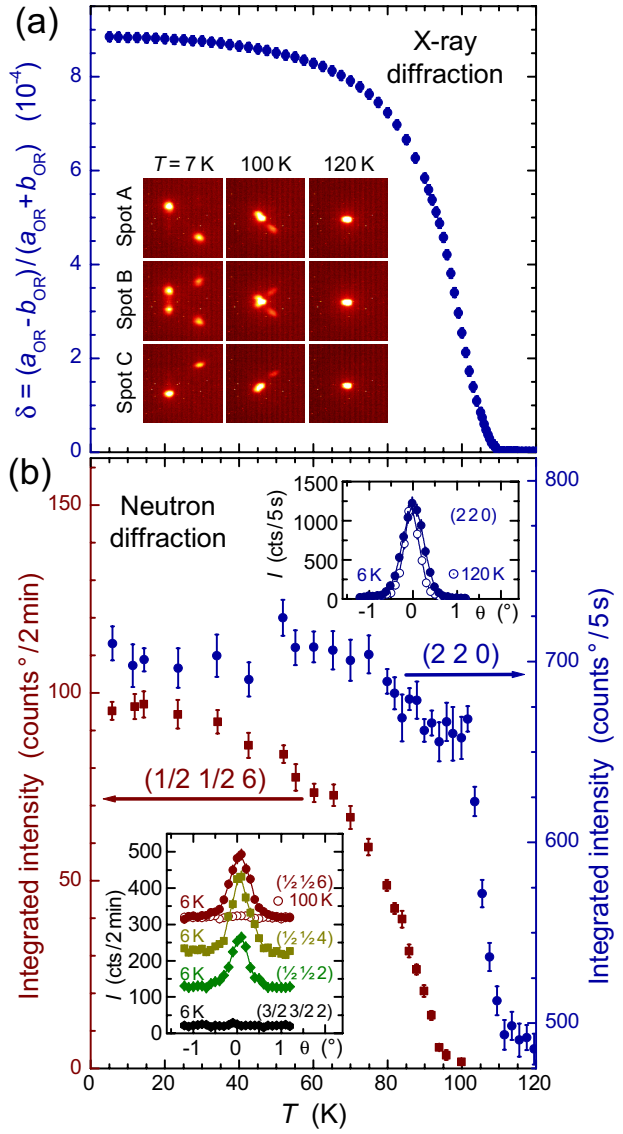

FIG. 2: (Color online) Temperature dependence of the order parameters of the $Ca_{10}(Pt_3As_8)(Fe_2As_2)_5$ single crystal. (a) Lattice distortion extracted from the high-resolution high-energy x-ray diffraction data shown in the inset measured at three different spots A-C on the sample in the surrounding of the (2 2 0) Bragg peak of the tetragonal body-centered base structure. The origin of the reciprocal space and the direct-beam direction is left from and far out of the shown detector area. (b) Integrated intensities of the antiferromagnetic $(\frac{1}{2}\ \frac{1}{2}\ 6)$ and nuclear (2 2 0) Bragg peaks measured in the neutron diffraction study of the $Ca_{10}(Pt_3As_8)(Fe_2As_2)_5$ single crystal. The insets show rocking scans through selected antiferromagnetic and nuclear Bragg peaks presented with intensity offsets for clarity.

distortion.[34] It is determined by extracting the in-plane orthorhombic lattice parameters a_{OR} and b_{OR} from the longitudinal splitting of the x-ray Bragg peaks near the (2 2 0) peak. The lattice distortion sets in below $T_S = 110(2)$ K as shown in Fig. 2(a) and reaches a maximum value of $\delta = 8.8(2)\times10^{-4}$, the same order of magnitude as observed in other Fe-based high-temperature superconductors.[34] The lattice distortion causes an increase of the nuclear (2 2 0) Bragg peak in the neutron diffraction study through an extinction release[35] below T_S as illustrated in Fig. 2(b), confirming consistent temperature scales for both scattering experiments performed on the same sample. The antiferromagnetic order sets in at $T_N = 96(2)$ K well below T_S as demonstrated by the temperature-dependent intensity of the antiferromagnetic $(\frac{1}{2}\ \frac{1}{2}\ 6)$ Bragg peak shown in Fig. 2(b). The temperature dependence is consistent with a continuous (or 2nd order) phase transition at T_N similar to the structural phase transition at T_S characterized by the lattice distortion δ shown in Fig. 2(a). This is also consistent with the lack of a step-like feature in the temperature-dependent curve of the distortion δ around T_N as observed in $BaFe_2As_2$ and derived compounds.[36]

Summarizing, $Ca_{10}(Pt_3As_8)(Fe_2As_2)_5$ is very similar to other Fe-based high-temperature superconductors not only in macroscopic physical properties, like the reported occurrence of superconductivity by partial element substitution of Fe by Pt, but also in its microscopic physical properties: Below $T_S = 110(2)$ K, the high-temperature square-like iron lattice gets distorted along its diagonal directions; below $T_N = 96(2)$ K, the Fe moments order in a long-range stripe-like antiferromagnetic structure built by Fe moments aligned and antiferromagnetically correlated along one of these directions and with ferromagnetic correlations perpendicular to it. Both transitions are continuous and well separated from each other. This similarity in physical properties is remarkable based on the observed strong differences in the chemical order: the Fe-As layers are much further separated from each other by Pt-As layers and neighboring Ca planes yielding a much more complex structure with lower crystal symmetry and severe chemical disorder in the sequence of the Pt-As layers. These intermediate layers modify the physical properties, *e. g.*, yielding only weak ferromagnetic interactions in the direction perpendicular to the layers;[18,20] however, major physical features seem very robust against variations of these intermediate layers in their chemical constitution as well as their structural perfection. These findings suggest that the Fe-As layer in tetragonal arrangement are key in determining the major physical properties of the class of Fe-based high-temperature superconductors.

The authors appreciate the help in sample preparation by M. G. Kim and W. Jayasekara, and the excellent support of the x-ray diffraction measurements by D. S. Robinson. Work at Ames Laboratory was supported by the U. S. Department of Energy, Office of Basic Energy Science, Division of Materials Sciences and Engineering. Ames Laboratory is operated for the U. S. Department of Energy by Iowa State University under Contract No. DE-AC02-07CH11358. The research conducted at Argonne National Laboratory and Oak

Ridge National Laboratory was sponsored by the U. S. Department of Energy, Office of Basic Energy Science, Scientific User Facilities Division. Work at Princeton University is supported by the Air Force Office of Scientific Research, Multidisciplinary University Research Initiative on Superconductivity.

[1] S. Kakiya, K. Kudo, Y. Nishikubo, K. Oku, E. Nishibori, H. Sawa, T. Yamamoto, T. Nozaka, and M. Nohara, J. Phys. Soc. Jpn. **80**, 093704 (2011).
[2] N. Ni, J. M. Allred, B. C. Chan, and R. J. Cava, Proc. Natl. Acad. Sci. USA **108**, E1019 (2011).
[3] C. Löhnert, T. Stürzer, M. Tegel, R. Frankovsky, G. Friederichs, and D. Johrendt, Angew. Chem. Int. Ed. **50**, 9195 (2011).
[4] T. Stürzer, G. Derondeau, and D. Johrendt, Phys. Rev. B **86**, 060516(R) (2012).
[5] M. Nohara, S. Kakiya, K. Kudo, Y. Oshiro, S. Araki, T. C. Kobayashi, K. Oku, E. Nishibori, and H. Sawa, Solid State Comm. **152**, 635 (2012).
[6] T. Tamegai, Q. P. Ding, T. Taen, F. Ohtake, H. Inoue, Y. Tsuchiya, S. Mohan, Y. Sun, Y. Nakajima, S. Pyon, and H. Kitamura, Physica C **494**, 65 (2013).
[7] K. Cho, M. A. Tanatar, H. Kim, W. E. Straszheim, N. Ni, R. J. Cava, and R. Prozorov, Phys. Rev. B **85**, 020504(R) (2012).
[8] Z. J. Xiang, X. G. Luo, J. J. Ying, X. F. Wang, Y. J. Yan, A. F. Wang, P. Cheng, G. J. Ye, and X. H. Chen, Phys. Rev. B **85**, 224527 (2012).
[9] Q.-P. Ding, Y. Tsuchiya, Y. Sun, T. Taen, Y. Nakajima, and T. Tamegai, J. Phys. Soc. Jpn. **81**, 114723 (2012).
[10] N. Ni, W. E. Straszheim, D. J. Williams, M. A. Tanatar, R. Prozorov, E. D. Bauer, F. Ronning, J. D. Thompson, and R. J. Cava, Phys. Rev. B **87**, 060507(R) (2013).
[11] J. S. Kim, T. Stürzer, D. Johrendt, and G. R. Stewart, J. Phys.: Condens. Matter **25**, 135701 (2013).
[12] P. Gao, L. Sun, N. Ni, J. Guo, Q. Wu, C. Zhang, D. Gu, K. Yang, A. Li, S. Jiang, R. J. Cava, and Z. Zhao, Adv. Mater. **26**, 2346 (2014).
[13] Y. Kobayashi, T. Iida, K. Suzuki, E. Satomi, T. Kawamata, M. Itoh, and M. Sato, J. Phys.: Conf. Ser. **400**, 022056 (2012).
[14] C. Hieke, J. Lippmann, T. Stürzer, G. Friederichs, F. Nitsche, F. Winter, R. Pöttgen, and D. Johrendt, Philos. Mag. **93**, 3680 (2013).
[15] K. Kudo, D. Mitsuoka, M. Takasuga, Y. Sugiyama, K. Sugawara, N. Katayama, H. Sawa, H. S. Kubo, K. Takamori, M. Ichioka, T. Fujii, T. Mizokawa, and M. Nohara, Sci. Rep. **3**, 3101 (2013).
[16] M. Neupane, C. Liu, S.-Y. Xu, Y.-J. Wang, N. Ni, J. M. Allred, L. A. Wray, N. Alidoust, H. Lin, R. S. Markiewicz, A. Bansil, R. J. Cava, and M. Z. Hasan, Phys. Rev. B **85**, 094510 (2012).
[17] H. Nakamura and M. Machida, Physica C **484**, 39 (2013).
[18] X. P. Shen, S. D. Chen, Q. Q. Ge, Z. R. Ye, F. Chen, H. C. Xu, S. Y. Tan, X. H. Niu, Q. Fan, B. P. Xie, and D. L. Feng, Phys. Rev. B **88**, 115124 (2013).
[19] S. Thirupathaiah, T. Stürzer, V. B. Zabolotnyy, D. Johrendt, B. Büchner, and S. V. Borisenko, Phys. Rev. B **88**, 140505(R) (2013).
[20] T. Berlijn, Phys. Rev. B **89**, 104511 (2013).
[21] M. Sato, T. Kawamata, Y. Kobayashi, Y. Yasui, T. Iida, K. Suzuki, M. Itoh, T. Moyoshi, K. Motoya, R. Kajimoto, M. Nakamura, Y. Inamura, and M. Arai, J. Phys.: Conf. Ser. **400**, 022105 (2012).
[22] K. Ikeuchi, M. Sato, R. Kajimoto, Y. Kobayashi, K. Suzuki, M. Itoh, P. Bourges, A. D. Christianson, H. Nakamura, M. Machida, unpublished, arXiv:1310.7424 (2013).
[23] T. Stürzer, G. M. Friederichs, H. Luetkens, A. Amato, H.-H. Klauss, and D. Johrendt, J. Phys.: Condens. Matter **25**, 122203 (2013).
[24] T. Zhou, G. Koutroulakis, J. Lodico, N. Ni, J. D. Thompson, R. J. Cava, and S. E. Brown, J. Phys.: Condens. Matter **25**, 122201 (2013).
[25] S. L. Bud'ko, N. Ni, and P. C. Canfield, Phys. Rev. B **79**, 220516(R) (2009).
[26] A. Kreyssig, S. Chang, Y. Janssen, J. W. Kim, S. Nandi, J. Q. Yan, L. Tan, R. J. McQueeney, P. C. Canfield, and A. I. Goldman, Phys. Rev. B **76**, 054421 (2007).
[27] M. A. Tanatar, A. Kreyssig, S. Nandi, N. Ni, S. L. Bud'ko, P. C. Canfield, A. I. Goldman, and R. Prozorov, Phys. Rev. B **79**, 180508(R) (2009).
[28] F. Nitsche, Th. Doert, M. Ruck, Solid State Sci. **19**, 162 (2013).
[29] M. A. Tanatar, E. C. Blomberg, A. Kreyssig, M. G. Kim, N. Ni, A. Thaler, S. L. Bud'ko, P. C. Canfield, A. I. Goldman, I. I. Mazin, and R. Prozorov, Phys. Rev. B **81**, 184508 (2010).
[30] E. C. Blomberg, A. Kreyssig, M. A. Tanatar, R. M. Fernandes, M. G. Kim, A. Thaler, J. Schmalian, S. L. Bud'ko, P. C. Canfield, A. I. Goldman, and R. Prozorov, Phys. Rev. B **85**, 144509 (2012).
[31] J. Zhao, Q. Huang, C. de la Cruz, S. Li, J. W. Lynn, Y. Chen, M. A. Green, G. F. Chen, G. Li, Z. Li, J. L. Luo, N. L. Wang, and P. Dai, Nat. Mater. **7**, 953 (2008).
[32] J. Zhao, Q. Huang, C. de la Cruz, J. W. Lynn, M. D. Lumsden, Z. A. Ren, J. Yang, X. Shen, X. Dong, Z. Zhao, and P. Dai, Phys. Rev. B **78**, 132504 (2008).
[33] W. Tian, W. Ratcliff II, M. G. Kim, J.-Q. Yan, P. A. Kienzle, Q. Huang, B. Jensen, K. W. Dennis, R. W. McCallum, T. A. Lograsso, R. J. McQueeney, A. I. Goldman, J. W. Lynn, and A. Kreyssig, Phys. Rev. B **82**, 060514(R) (2010).
[34] S. Nandi, M. G. Kim, A. Kreyssig, R. M. Fernandes, D. K. Pratt, A. Thaler, N. Ni, S. L. Bud'ko, P. C. Canfield, J. Schmalian, R. J. McQueeney, and A. I. Goldman, Phys. Rev. Lett. **104**, 057006 (2010).
[35] A. Kreyssig, M. G. Kim, S. Nandi, D. K. Pratt, W. Tian, J. L. Zarestky, N. Ni, A. Thaler, S. L. Bud'ko, P. C. Canfield, R. J. McQueeney, and A. I. Goldman, Phys. Rev. B **81**, 134512 (2010).
[36] M. G. Kim, R. M. Fernandes, A. Kreyssig, J. W. Kim, A. Thaler, S. L. Bud'ko, P. C. Canfield, R. J. McQueeney, J. Schmalian, and A. I. Goldman, Phys. Rev. B **83**, 134522 (2011).